Contents lists available at ScienceDirect

Scripta Materialia

journal homepage: www.elsevier.com/locate/scriptamat



Stress-driven grain refinement in a microstructurally stable nanocrystalline binary alloy



K.A. Darling ^{a,*}, S. Srinivasan ^b, R.K. Koju ^c, B.C. Hornbuckle ^a, J. Smeltzer ^{a,d}, Y. Mishin ^c, K.N. Solanki ^{b,*}

- ^a Army Research Laboratory, Weapons and Materials Research Directorate, APG, MD, 21014, USA
- ^b School for Engineering of Matter, Transport, and Energy, Arizona State University, Tempe, AZ, 85287, USA
- ^c Department of Physics and Astronomy, George Mason University, MSN 3F3, Fairfax, VA 22030, USA
- ^d Department of Materials Science and Engineering, Lehigh University, 5 E Packer Ave, Bethlehem, PA, 18015, USA

ARTICLE INFO

Article history: Received 20 August 2020 Revised 23 September 2020 Accepted 24 September 2020 Available online 4 October 2020

Keywords: Nanocrystalline material Grain refinement Thermally stable Recrystallization

ABSTRACT

Deformation-induced grain-growth in nanocrystalline materials is a widely-reported phenomenon that has been attributed to grain boundary (GB) processes. In this paper, we report on the opposite phenomenon, wherein a stable nanocrystalline (NC) Cu-Ta alloy undergoes a further refinement of the nanograins during severe plastic deformation (SPD). SPD up to 250% results in a significant grain-size reduction despite the 350°C increase in temperature caused by the deformation process. Experiments and atomistic-simulations show that this unexpected grain-refinement is a direct result of well-dispersed Tananoclusters throughout grain centers and along GBs acting as kinetic-pinning agents and suppressing GB processes that occur during recrystallization.

 $\ensuremath{\mathbb{C}}$ 2020 Acta Materialia Inc. Published by Elsevier Ltd. All rights reserved.

Severe plastic deformation (SPD) by machining or friction stir processing (FSP) has been shown to induce grain refinement in coarse-grained materials down to sub-micrometer or nanometer grain sizes [1–6]. For instance, deformation rates during machining are on the order of 10^3 s⁻¹ or higher. Approximately 98% of the energy dissipated in the material during deformation manifests itself as heat, causing a localized increase in temperature of up to several hundred degrees [7]. Under these extreme conditions (i.e. high temperature, high pressure, and intense friction) localized regions near the tool-chip interface experience structural refinement in the surface layer via the process of dynamic recrystallization [6]. While grain refinement can be attained, a lower bound of average grain size that can be achieved through this process exists given that the grain refinement by deformation is often accompanied by concurrent thermally activated grain growth, also known as deformationinduced grain growth [1,2,5].

Deformation-induced grain growth is a widely reported phenomenon, especially in NC materials, and has been observed during uniaxial tension testing [2,8,9], fatigue [10], and other mechanical tests performed under cryogenic temperatures [3]. For example, Gianola et al. [8], through tensile experiments on NC Al

E-mail addresses: kristopher.a.darling.civ@mail.mil (K.A. Darling), Kiran.solanki@asu.edu (K.N. Solanki).

have demonstrated stress-driven grain growth of about ~2.5 times the as-deposited grain size (from 38nm to 92nm). Similar stressinduced grain growth was observed by Fan et al. [9] during uniaxial compression of NC-Ni-Fe thin films. Cyclic deformation of a NC-Ni-Mn alloy also resulted in grain growth from an initial grain size of 115 nm to about micron-size grains along the fatigue crack [10]. Additionally, rapid grain coarsening, from 20 nm to about 200-300 nm (almost 10 fold the initial grain size), has been reported as a result of room and cryogenic temperature indentation experiments on NC-Cu [3]. High-pressure torsion (HPT) and highenergy ball milling have also been shown to induce grain growth in NC materials [5,11]. For example, Liao et al. [12] and Wang et al. [5] have reported final grain sizes about 5-to-10 times that of the initial grain size in NC-Ni and Ni-Fe alloys, respectively, as a result of HPT and mechanical alloying. In all of the aforementioned studies, deformation-induced grain growth has been attributed to GB processes such as shear-coupled GB-motion [13], GB-sliding, and grain rotation [2,3,14,15].

While it is clear some NC systems readily experience grain growth, others, such as NC-Cu-Ta, have shown exceptional thermal [16] and thermomechanical stability [17–25]. This raises the following questions: Does the deformation-induced grain growth mentioned above also occur in thermo-mechanically stable NC materials such as Cu-Ta alloys? If not, can such materials exhibit grain refinement instead of grain growth? If they can, what are

^{*} Corresponding authors.

the mechanisms of this unusual behavior? To answer these questions, we first use uniaxial compression experiments at two different temperatures to demonstrate the thermo-mechanical stability of a NC-Cu-Ta alloy chosen for this study. We then deform the material in the SPD mode by machining and apply advanced electron microscopy to characterize and compare the microstructural features before and after the deformations. These experiments are integrated with atomistic computer simulations capable of providing insight into the microscopic mechanisms responsible for the observed grain refinement process.

A NC-Cu-based alloy containing 3at.%Ta (hereafter designated as Cu-3Ta alloy) was chosen for the study. The alloy rod was produced from mechanically alloyed powders using a multi-pass hightemperature equal channel angular extrusion (ECAE) canning operation that resulted in a total strain of 460% at 700°C. Complete details of the powder processing and consolidation can be found in [20,22]. Cylindrical compression specimens 3mm in height and 3mm in diameter were fabricated from the ECAE processed rod via electric discharge machining. Compression tests were performed using an INSTRON load frame with a 50 kN load capacity and a furnace rated up to 1373K. Boron nitride lubricated polished WCdisks were used as platens. The test setup was preheated to the required testing temperature for about 30 minutes to attain equilibrium and thermocouples were attached to the specimen to monitor the temperature. The specimens were then loaded under a strain control with a strain rate of 0.001 s^{-1} . To achieve SPD by machining, a cylindrical rod of Cu-3Ta 8mm in diameter was turned on a Haas ST10 CNC lathe using a Sandvik CNMG 12 04 08-PM 4325 cutting insert with a cutting speed of 84cm/s (2000rpm), a feed rate of 0.08 mm per revolution, and a cutting depth of 0.130 mm per pass to reveal the consolidated Cu-3Ta rod from ECAE process. Then, using a Carmex 11 ER AGO BMA single-point, external insert operating at a cutting speed of 120cm/s (3000 rpm), a feed rate of 0.94 mm per revolution, and a 60° lead-in angle, SPD was induced. The microstructure of the material was characterized by transmission electron microscopy (TEM) using a JEOL 2100F and JEOL ARM 200F operated at 200kV. TEM samples postcompression were prepared using conventional dimpling and ion milling to electron transparency using a GATAN PIPS ion mill system while post-machined specimens were prepared using an FEI Nova600i Nanolab dual-beam focused ion beam (FIB)/SEM.

Atomic interactions in the Cu-Ta system were described with a well-tested angular-dependent interatomic potential [26]. Molecular dynamics (MD) and Monte Carlo (MC) simulations utilized the LAMMPS [27] and ParaGrandMC [28] codes, respectively. Visualization of the atomic structures was performed using the software package OVITO [29]. A polycrystalline Cu sample containing 5.4 million atoms was composed of 32 randomly oriented grains constructed by the Voronoi tessellation method. The average grain size was about 10 nm. The GB structures were optimized by a procedure described elsewhere [26,30]. The atoms in the grains were automatically identified and tracked using a parallelized C++ computer code written for this work. The lattice orientation in the neighborhood of each atom was determined from the orientation of neighboring atoms relative to a reference FCC unit cell, similar to the method described in [31]. Atoms lying in GBs were identified using the centrosymmetry parameter and the bond-angle analysis [29] and were excluded from the grain orientation analysis. Once the orientation is determined, the excluded atoms were revisited, and some of them were counted as grain atoms if 90% of their neighbors lying within 1 nm radius had the same orientation. Grains were considered different if their misorientation angles exceeded 4°. Equilibrium distribution of 3at.% of Ta atoms were created by a composition-controlled semi-grand canonical MC algorithm [32] at the temperature of 673K. Note that both the alloy composition and temperature match the experimental values. The simulations were performed for both the Cu-3Ta alloy and for pure Cu used as a reference system.

Microstructural analysis (Fig. 1A-C) indicates that the asextruded alloy has an average grain size of 99nm. Statistical analysis of Fig. 1B shows the presence of an extremely dense network of Ta nanoclusters with a mean diameter of 2nm located both within the grains and along GBs, which is consistent with previous works [19,20,23,33]. It has been previously determined that the Ta nanoclusters play an important role in dictating the mechanical response and in stabilizing the grain size under the application of stress and temperature during processing and mechanical testing [16,18,19,23]. Thermo-mechanical stability of the Cu-3Ta alloy was first tested by conventional quasi-static compression experiments at 298K and 673K. Fig. 1D shows the compression true stress-strain responses of the alloy, which reveal significant findings. Firstly, the absence of appreciable strain hardening (i.e., near elastic-perfectly plastic behavior) at both temperatures suggests the absence of significant changes in the grain morphology or texture during the deformation. Secondly, the 0.2% yield strength at 298K and 673K was found to be about 920MPa and ~600 MPa, respectively, which is significantly higher than that reported for NC-Cu [34]. Overall, the strength of the NC-Cu-3Ta alloy at $50\%T_m$ is more than six times the strength of pure polycrystalline Cu and the threetimes the strength of brass at 298K [34,35]. TEM micrographs of the post deformed samples are shown in Fig. 1E-H. Lower magnification images (Fig. 1E,G) indicate that the material still maintains its NC microstructure. Higher magnification images show the small Ta clusters decorating the grain interior as well as the GBs (Fig. 1F,H), which strongly retard the grain growth by the Zener pinning mechanism and impart thermo-mechanical stability to the alloy at higher temperatures [16,18,19,23].

Subsequently, the effect of SPD through machining on the microstructure was studied using a TEM lift out from the machined surface. The microstructure of the machined surface (Fig. 2A) with statistical analysis (Fig. 2B) reveals that the average grain size is ~37nm, which is approximately one-third of the starting (as-ECAE) grain size. This result is contrary to what would be normally expected. Significant grain growth observed in bulk NC materials as a result of SPD [12] can be explained by processes such as shearcoupled GB migration in deformation-induced shear bands. Due to the local temperature rise, the heavily deformed microstructure can also undergo dynamic recrystallization inducing grain growth. By contrast, in the NC-Cu-Ta alloys, the pinning of the newly formed GBs by the Ta clusters slows down or even suppresses the grain growth, thus resulting in grain refinement instead of grain growth. The situation is similar to that in the original ball milling process, which is known to produce grain sizes as small as 10 nm or less in Cu-Ta alloys. That is, the clusters derived and stochastically distributed throughout the interior of the Cu grains via previous processing are so stable that they can be used as a template during SPD to restore the microstructure in a rejuvenation process yielding a final refined end state. Note that the processing of machining chips through a ball milling would further reduce the grain size. Nevertheless, this restoring process, in equilibrium phase separating Cu-Ta alloys, was reported previously for various other aspects of their microstructure but under different stimuli [36]. For example, intense irradiation has been shown to precipitate additional Ta nanoclusters, greatly increasing the alloy stability against further irradiation damage and the anomalous ability to resist/distribute and/or absorb damage accumulation during high rate and shock loading events [24,37,38], leaving the grains relatively free of dislocations and or other defects.

Atomistic simulations were performed to support the experimental findings and gain further insights into the grain refinement mechanisms. SPD modeling of the alloy was achieved by the application of extremely large shear deformation. To this end, the simu-

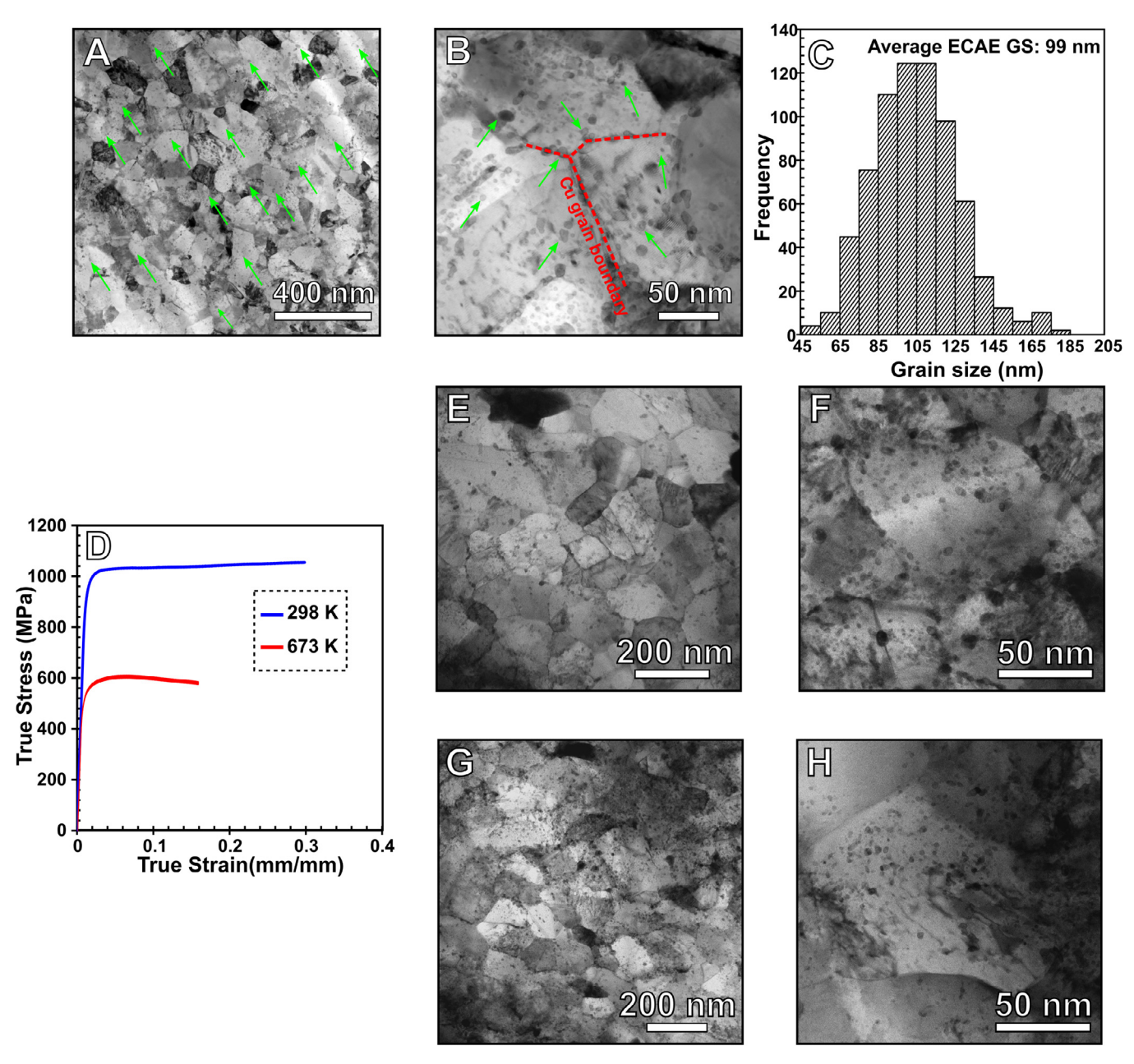


Fig. 1. (A-C) As-received (i.e. post-ECAE processed) NC-Cu-Ta characterization: (A) Low magnification BF STEM image showing grain structure and small Ta clusters indicated by green arrows. (B) High magnification image showing the high density of Ta clusters residing in the grains and along GBs. (C) Grain size distribution. (D-I) Thermomechanical characterization: (D) Compression true stress-strain response at two different temperatures showing near elastic perfectly plastic behavior without apparent strain hardening. Low and high magnification STEM BF images of compressed Cu-3Ta alloy (E)-(F) at 298 K and (G)-(H) at 673 K.

lation block was clamped between two 1.5nm thick rigid layers (refer to Fig. 2C). The system was pre-expanded to reach the equilibrium lattice constant at the chosen temperature to eliminate thermal stresses during the simulations. The MD ensemble was NVT (constant temperature and volume) with a Nose/Hoover thermostat. After equilibrating the system for 0.5ns, the shear stress was applied by keeping the lower layer fixed and moving the upper layer as a rigid body with a constant translation velocity of 1m/s in the horizontal direction (Fig. 2C). This produced SPD on the material in the shear mode up to 250%. Stress-strain curves obtained from the simulations in Fig. 2D indicate higher flow stress for Cu-3Ta than for Cu as expected. The initial stress peak is due to the dislocation-free initial state of the material. Once a sufficient number of defects is accumulated, the deformation process continues under nearly constant flow stress. Fig. 2E-F compares the grain size

distributions before and after the 250% shear deformation at 673K. The grain size is defined by $(n\Omega)^{1/3}$, where Ω is the atomic volume and n is the number of atoms in the grain. In pure Cu, the average grain size changes from 10 ± 3 to 9 ± 4 nm, i.e., remains the same within the error bar. However, the total number of grains decreases, and the shape of the distribution changes. After the SDP, the distribution becomes nearly bimodal, with large grain sizes extending significantly beyond the upper bound of the initial distribution while many other grains shrink to smaller sizes. By contrast, in Cu-3Ta the average grain size decreases from 10 ± 4 nm to 6 ± 3 nm. Furthermore, as shown in Fig. 2F, the new distribution displays a high peak at grain sizes around 4-5 nm, which is less than 50% of the initial grain size.

The changes in the microstructure due to the SPD are further illustrated in Fig. 3. The image in Fig. 3B shows that the SPD of Cu

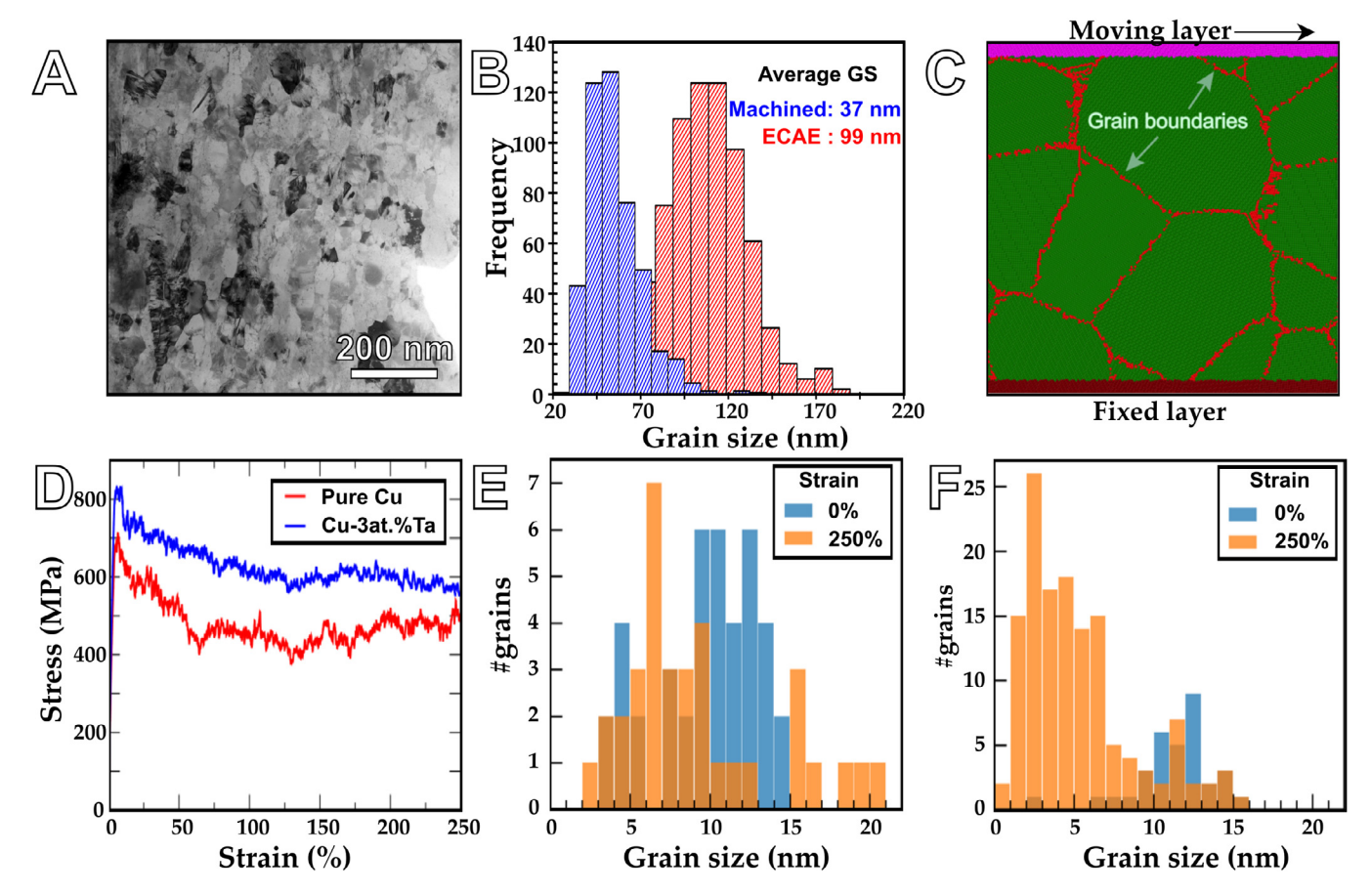


Fig. 2. (A) TEM microstructure of the machined surface (B) Grain size distribution comparison (before and after SPD). (C) Cross-section of the simulation block used for SPD modeling. The material is attached to two parallel layers. The lower layer is fixed while the upper layer moves to the right producing shear deformation. (D) Shear stress vs shear strain for pure Cu and the Cu-3Ta alloy. (E-F) Grain size distribution in (E) pure Cu and (F) Cu-3Ta before and after severe shear deformation by 250%. The results were obtained by MD simulations at a temperature of 673 K.

causes the formation of large grains coexisting with a collection of small grains mostly located next to the fixed regions. Few dislocations are observed, suggesting easy glide across the nano-grains. In the deformed Cu-3Ta alloy, the grains are visibly smaller and tend to be elongated parallel to the shear directions. The grain shapes are irregular with many GBs becoming rough and/or serrated. This serrated or step morphology of GBs after interaction with Ta clusters has been recently captured by aberration-corrected STEM imaging [39]. The dislocation density is much higher than in pure Cu. Closer examination shows that many dislocations attempting to glide across the nano-grains were stopped by the Ta clusters. Analysis of the deformation process in time reveals that the Ta clusters play a critical role in the grain refinement. One of the typical refinement mechanisms was grain fragmentation. The dislocations arrested by the clusters had a highly non-uniform distribution in the microstructure. They occasionally created a high dislocation density in certain regions inside a grain, while the rest of the grain had a lower dislocation density. This eventually resulted in the reconstruction of the dislocations into a wall separating the high and low-density domains in two differently oriented grains. Deformation twinning was frequently observed, with twin boundaries typically originating from high-angle GBs. All these processes are accompanied by only a moderate amount of GB sliding and grain rotation operating as shape accommodation mechanisms. As in pure Cu, the grains attached to the fixed layers were partitioned into the smaller grain strongly elongated parallel to the shear direction. These grains were subjected to more severe geometric constraints than the inner grains, resulting in higher dislocation densities. The mechanisms described here are illustrated in more detail in additional images and animations included in the supplementary file accompanying this paper.

In conclusion, we have reported on an unusual phenomenon wherein a NC material undergoes a significant refinement of the nanograins under SPD conditions at an elevated temperature. This behavior is contrary to the commonly observed grain growth caused by the deformation of NC materials and may result in enhanced wear and fatigue resistance. The material exhibiting this deformation-induced grain refinement is a NC-Cu-Ta alloy whose microstructure is strongly stabilized by a distribution of Ta nanoclusters. Both experiments and complementary atomistic simulations show that the nanoclusters prevent the grain-growth by pinning the GBs and arresting lattice dislocations. These pinning processes strongly stabilize the nanostructure and block the grain growth mechanisms that normally operate in other NC materials under SPD conditions, such as shear-coupled GB-migration, GB-sliding, and grain rotation. Furthermore, by arresting the dislocations inside the grains, the Ta clusters create a high dislocation density that drives processes such as grain fragmentation and dynamic recrystallization, while simultaneously restraining the growth of new grains. As a result, a 250% SPD of the NC-Cu-Ta alloy by machining causes a significant reduction in the grain size despite the increase in temperature due to the heat released during the deformation. Overall, the family of immiscible NC-Cu-Ta alloys has proven their ability to restore various aspects of their microstructures in an almost rejuvenation like process including the Ta clusters and cluster densities, defect-free grain interiors, and

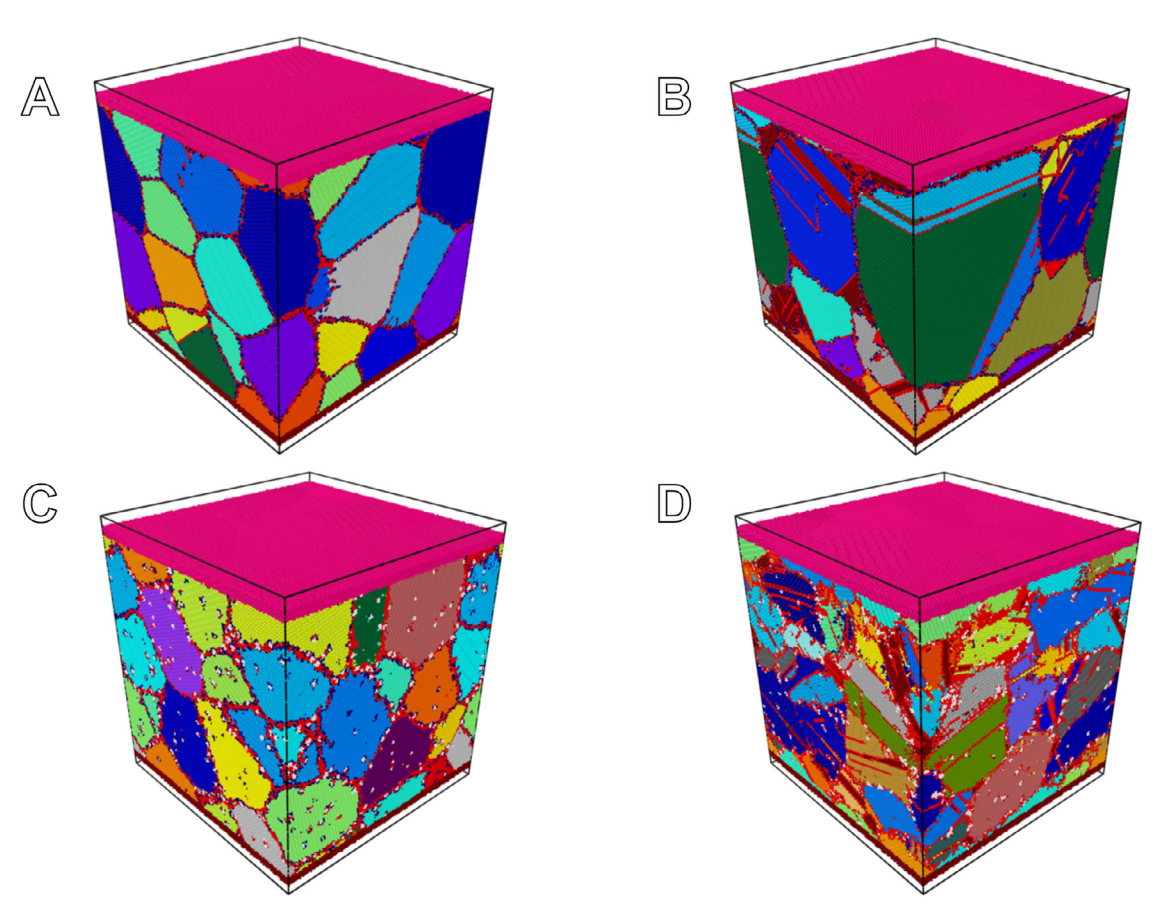


Fig. 3. Comparison of the structures of (A,B) pure Cu and (C,D) Cu-3Ta alloy before (A,C) and after (B,D) severe shear deformation to 250% strain at the temperature of 673 K. The grains are colored according to lattice orientation. The GB, HCP, and other structural atoms are colored in red. Ta clusters are colored in white.

now the matrix grain size itself [36]. The inherent immiscibility of these nanostructured Cu-Ta alloys puts them among the most resilient alloys known.

Declaration of Competing Interest

The authors declare that they have no known competing financial interests or personal relationships that could have appeared to influence the work reported in this paper.

Acknowledgments

S.S. and K.N.S. acknowledge the support of the US Army Research Laboratory under contract W911NF-15-2-0038 and a National Science Foundation grant No. 1663287. S.S. and K.N.S. acknowledge the use of facilities within the Eyring Materials Center at Arizona State University supported in part by NNCI-ECCS-1542160. R. K. K and Y. M. were supported by the U.S. Army Research Office under contract number W911NF-15-1-007.

Supplementary materials

Supplementary material associated with this article can be found, in the online version, at doi:10.1016/j.scriptamat.2020.09. 041.

References

- [1] R.S. Mishra, Z.Y. Ma, Mater. Sci. Eng. R Rep 50 (2005) 1-78.
- [2] T.J. Rupert, D.S. Gianola, Y. Gan, K.J. Hemker, Science 326 (2009) 1686–1690. [3] K. Zhang, J.R. Weertman, J.A. Eastman, Appl. Phys. Lett 87 (2005) 061921.
- [4] C.I. Chang, X.H. Du, J.C. Huang, Scr. Mater 57 (2007) 209-212.

- [5] Y.B. Wang, J.C. Ho, X.Z. Liao, H.Q. Li, S.P. Ringer, Y.T. Zhu, Appl. Phys. Lett 94 (2009) 011908
- [6] M.R. Shankar, S. Chandrasekar, A.H. King, W.D. Compton, Acta Mater 53 (2005) 4781-4793
- [7] E.M. Trent, P.K. Wright, Metal Cutting, Butterworth-Heinemann, 2000.
- [8] D.S. Gianola, S. Van Petegem, M. Legros, S. Brandstetter, H. Van Swygenhoven, K.J. Hemker, Acta Mater 54 (2006) 2253-2263.
- [9] G.J. Fan, Y.D. Wang, L.F. Fu, H. Choo, P.K. Liaw, Y. Ren, N.D. Browning, Appl. Phys. Lett 88 (2006) 171914.
- [10] H.A.P. Ii, B.L. Boyce, Exp. Mech. 50 (2010) 5-23
- [11] T.R. Malow, C.C. Koch, Acta Mater 45 (1997) 2177–2186.
- [12] X.Z. Liao, A.R. Kilmametov, R.Z. Valiev, H. Gao, X. Li, A.K. Mukherjee, J.F. Bingert, Y.T. Zhu, Appl. Phys. Lett 88 (2006) 021909.
- [13] J.W. Cahn, Y. Mishin, A. Suzuki, Acta Mater 54 (2006) 4953-4975
- J.A. Sharon, P.-C. Su, F.B. Prinz, K.J. Hemker, Scr. Mater 64 (2011) 25-28.
- V. Yamakov, D. Wolf, S.R. Phillpot, A.K. Mukherjee, H. Gleiter, Nat. Mater 3 (2004) 43-47.
- [16] K.A. Darling, A.J. Roberts, Y. Mishin, S.N. Mathaudhu, L.J. Kecskes, J. Alloys Compd 573 (2013) 142-150.
- K.A. Darling, M.A. Tschopp, R.K. Guduru, W.H. Yin, Q. Wei, L.J. Kecskes, Acta Mater 76 (2014) 168-185. [18] K.A. Darling, E.L. Huskins, B.E. Schuster, Q. Wei, L.J. Kecskes, Mater. Sci. Eng. A
- 638 (2015) 322-328.
- [19] K.A. Darling, M. Rajagopalan, M. Komarasamy, M.A. Bhatia, B.C. Hornbuckle, R.S. Mishra, K.N. Solanki, Nature 537 (2016) 378-381.
- [20] B.C. Hornbuckle, T. Rojhirunsakool, M. Rajagopalan, T. Alam, G.P.P. Pun, R. Banerjee, K.N. Solanki, Y. Mishin, L.J. Kecskes, K.A. Darling, JOM 67 (2015) 2802-2809.
- [21] R.K. Koju, K.A. Darling, K.N. Solanki, Y. Mishin, Acta Mater 148 (2018) 311-319.
- [22] K.A. Darling, C. Kale, S. Turnage, B.C. Hornbuckle, T.L. Luckenbaugh, S. Grendahl, K.N. Solanki, Scr. Mater 141 (2017) 36-40.
- [23] M. Rajagopalan, K. Darling, S. Turnage, R. Koju, B. Hornbuckle, Y. Mishin, K. Solanki, Mater. Des 113 (2017) 178-185.
- [24] S.A. Turnage, M. Rajagopalan, K.A. Darling, P. Garg, C. Kale, B.G. Bazehhour, I. Adlakha, B.C. Hornbuckle, C.L. Williams, P. Peralta, K.N. Solanki, Nat. Commun 9 (2018) 2699.
- [25] M. Rajagopalan, K.A. Darling, C. Kale, S.A. Turnage, R.K. Koju, B.C. Hornbuckle, Y. Mishin, K.N. Solanki, Mater. Today 31 (2019) 10-20.
- [26] G.P. Purja Pun, K.A. Darling, L.J. Kecskes, Y. Mishin, Acta Mater 100 (2015)

- [27] S. Plimpton, J. Comput. Phys 117 (1995) 1–19.

- [27] S. Pilmpton, J. Comput. Phys 117 (1995) 1–19.
 [28] V.I. Yamakov, (2016).
 [29] A. Stukowski, Model. Simul. Mater. Sci. Eng 18 (2009) 015012.
 [30] Z.T. Trautt, A. Adland, A. Karma, Y. Mishin, ArXiv12063549 Cond-Mat (2012).
 [31] J.F. Panzarino, T.J. Rupert, JOM 66 (2014) 417–428.
 [32] Y. Mishin, Model. Simul. Mater. Sci. Eng 22 (2014) 045001.
 [33] M. Bhatia, M. Rajagopalan, K. Darling, M. Tschopp, K. Solanki, Mater. Res. Lett 5 (2017) 48–56. 5 (2017) 48-54.
- [34] M.A. Meyers, A. Mishra, D.J. Benson, Prog. Mater. Sci 51 (2006) 427–556.
 [35] M.A. Meyers, K.K. chawla, Mechanical Behavior Materials, 2nd ed., Cambridge University Press, United Kingdom, 2008.
- [36] S. Srinivasan, C. Kale, B.C. Hornbuckle, K.A. Darling, M.R. Chancey, E. Hernández-Rivera, Y. Chen, T.R. Koenig, Y.Q. Wang, G.B. Thompson, K.N. Solanki, Acta Mater 195 (2020) 621–630.
- Mater 195 (2020) 621–630.
 [37] B.C. Hornbuckle, C.L. Williams, S.W. Dean, X. Zhou, C. Kale, S.A. Turnage, J.D. Clayton, G.B. Thompson, A.K. Giri, K.N. Solanki, K.A. Darling, Commun. Mater 1 (2020) 1–6.
 [38] B.C. Hornbuckle, S.W. Dean, X. Zhou, A.K. Giri, C.L. Williams, K.N. Solanki, G.B. Thompson, K.A. Darling, Appl. Phys. Lett 116 (2020) 231901.
 [39] T. Meiners, J.M. Duarte, G. Richter, G. Dehm, C.H. Liebscher, Acta Mater 190 (2020) 93–104.